Effects of the chemical bonding on the optical and mechanical properties for germanium carbide films used as antireflection and protection coating of ZnS windows

2006 J. Phys.: Condens. Matter 18 4231

(http://iopscience.iop.org/0953-8984/18/17/011)

INSTITUTE OF PHYSICS PUBLISHING JOURNAL OF PHYSICS: CONDENSED MATTER

J. Phys.: Condens. Matter **18** (2006) 4231–4241 doi:10.1088/0953-8984/18/17/011

Effects of the chemical bonding on the optical and mechanical properties for germanium carbide films used as antireflection and protection coating of ZnS windows

Chaoquan Hu, Weitao Zheng[1], Hongwei Tian, Le Xu and Qing Jiang

Department of Materials Science and Key Laboratory of Automobile Materials of MOE, Jilin University, Changchun 130012, People's Republic of China

E-mail: WTZheng@jlu.edu.cn

Received 6 March 2006
Published 13 April 2006
Online at stacks.iop.org/JPhysCM/18/4231

Abstract

Germanium carbide ($Ge_{1-x}C_x$) films have been prepared by RF reactive sputtering a pure Ge(111) target at different flow rate ratios of $CH_4/(CH_4 + Ar)$ in a CH_4/Ar mixture discharge, and it has been found that the composition, chemical bonding, optical and mechanical properties of $Ge_{1-x}C_x$ films are remarkably influenced by the flow rate ratio of $CH_4/(CH_4 + Ar)$. The effects of the chemical bonding on the optical and mechanical properties of the $Ge_{1-x}C_x$ films have been explored. In addition, an antireflection $Ge_{1-x}C_x$ double-layer coating deposited on both sides of the ZnS substrate wafer has been developed for application as an infrared window. It is shown that the transmittance in the wavelength region between 8 and 12 μm and the hardness of the ZnS substrate have been significantly improved by the double-layer coating.

1. Introduction

An increasing number of military applications in recent years are associated with high velocity windows operating in the 8–12 μm thermal band. The high temperatures caused by aerodynamic heating in these instances preclude the use of germanium with its relatively low bandgap (0.7 eV) due to absorption becoming excessive above 100 °C. Zinc sulfide, with a bandgap around 3.6 eV, is currently the preferred material. However, concerning the applications of zinc sulfide for an infrared window, there are two major deficiencies as follows: (1) zinc sulfide is relatively soft and brittle, and often degrades when subjected to a particle-impacting environment [1]; (2) the refractive index of zinc sulfide is as high as 2.3, resulting in a reflection of 15.5% from a single surface and of 27% for a slab allowing for multiple reflections.

[1] Author to whom any correspondence should be addressed.

These deficiencies preclude the direct use of bare zinc sulfide for an infrared window and urge us into developing the durable antireflection and protection coating on ZnS substrate in order to improve the poor optical and mechanical properties of ZnS window.

Germanium carbide ($Ge_{1-x}C_x$) films have numerous attractive properties, such as low stress and light absorption, and good adhesion on many infrared substrates such as ZnS and Ge. In particular, the refractive index can be widely varied, with composition within the range of 2–4. This excellent performance makes $Ge_{1-x}C_x$ films promising candidates for applications in the field of multilayer antireflection and protection coating of IR windows. Up to the present, some optical, electrical, and structural properties have already been reported for the $Ge_{1-x}C_x$ film prepared, under different conditions, by chemical vapour deposition [2, 3], activated reactive evaporation (ARE) [4, 5], glow discharge [6, 7], reactive sputtering of either germanium in hydrocarbon atmosphere [8, 9] or mixed germanium/carbon targets in hydrogen and/or argon atmosphere [10–12]. However, there have been very few reports about the influence of deposition parameter on the chemical bonding of $Ge_{1-x}C_x$ films; in particular, the correlation between chemical bonding and optical and mechanical properties of $Ge_{1-x}C_x$ films has not been referred to in the literature. In addition, as regards the application of the $Ge_{1-x}C_x$ films for antireflection and protection coating of the IR ZnS window, the desired IR transmission performance has not been achieved, though the mechanical properties of ZnS substrates overcoated by these durable $Ge_{1-x}C_x$ coatings have been significantly improved [13, 14].

In this work, the $Ge_{1-x}C_x$ films have been prepared by RF reactive sputtering a pure Ge(111) target in a CH_4/Ar mixture discharge, and their chemical bonding, optical and mechanical properties have been investigated as a function of the flow rate ratios of $CH_4/(Ar + CH_4)$. The effects of the chemical bonding on the optical and mechanical properties of the $Ge_{1-x}C_x$ films have been explored. Furthermore, a $Ge_{1-x}C_x$ double-layer coating on ZnS substrate for the application as an infrared window, deposited using RF reactive sputtering, has been developed in order to increase the optical transmittance of ZnS substrate in the wavelength region of 8–12 μm.

2. Experimental details

The $Ge_{1-x}C_x$ films were simultaneously deposited both on single-crystal Si(001) and on polycrystalline ZnS substrates using RF magnetron sputtering [15] and a single-crystal Ge(111) target (100 mm in diameter and 3 mm in thickness). The distance between the target and substrate holder was fixed at 80 mm. The chamber was evacuated by turbomolecular pump to 6×10^{-4} Pa prior to film deposition. Before being introduced into the vacuum chamber, the Si and ZnS substrates were cleaned ultrasonically in acetone and petroleum ether, consecutively.

The $Ge_{1-x}C_x$ films were synthesized in the mixed discharge gases of Ar (99.99%) and CH_4 (99.99%). During the deposition, the RF power and substrate temperature were kept at 150 W and 200 °C, respectively. The flow rate of Ar and CH_4 was accurately controlled by a D08-1A/ZM mass flow controller. When the gas flow rate ratio (R) of $CH_4/(Ar + CH_4)$ was varied from 0 to 100%, the work pressure was always kept at 1.0 Pa. $Ge_{1-x}C_x$ films were deposited on single-crystal silicon substrate for most measurements, only for IR transmittance measurement ZnS substrate is used. X-ray diffraction experiments showed that all samples were amorphous. They exhibited good adhesion and stability on Si and ZnS substrates.

XPS measurements were performed using a monochromatized Mg Kα (1253.6 eV) x-ray source with an energy resolution of 0.5 eV (VG ESCALAB MK II). Prior to XPS analyses, argon ion cleaning lasting 120 s was accomplished by 5 keV ion beam energy for all samples. The Raman spectra were obtained using a laser confocal Raman spectrometer with an Ar^+

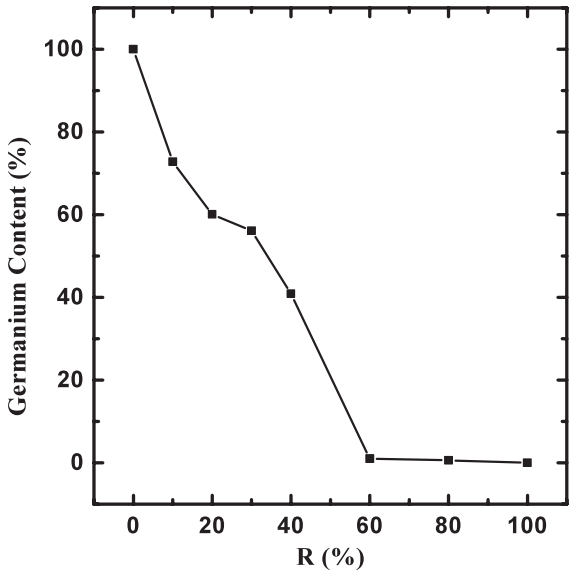

Figure 1. The germanium content for the $Ge_{1-x}C_x$ films as a function of the flow rate ratio (R) of $CH_4/(CH_4 + Ar)$.

(514.5 nm) laser, made by Renishaw, UK. The IR transmittance in the range of 4000–400 cm^{-1} was measured by employing a Perkin Elmer Spectrum One B type Fourier transform infra-red (IR) spectrometer, and the spectra were recorded at a resolution of 4 cm^{-1}. Film thickness was measured with a Dektak^3 surface profile measuring system. The refractive indices and extinction coefficients of samples were determined using a M-2000 variable angle incidence spectroscopic ellipsometer (VASE) made by Woollam, and the VASE data were acquired at four angles of incidence (55°, 60°, 65° and 70°) over the spectral range of 250–1700 nm. Hardness measurements were performed using micro-Vickers test equipment with a diamond indentation.

3. Results and discussion

3.1. Composition and chemical bonding

Figure 1 shows the germanium content of the $Ge_{1-x}C_x$ thin films determined by XPS as a function of the gas flow rate ratio (R) of $CH_4/(Ar + CH_4)$. As expected, the germanium content decreases with the increase of the R. This is because that the Ge target is sputtered mainly by argon ions rather than by a species with a small sputtering yield such as hydrogen ions and hydrocarbon ions decompose from methane [16]. When the flow rate ratio increases with the work pressure and RF power keeps constant, the argon partial pressure decreases and the number of argon ions in plasma reduces, which leads to a decrease in germanium content of the $Ge_{1-x}C_x$ films. However, an abrupt decrease of germanium content ($<1\%$) is observed with $R > 40\%$, which is due to occurrence of the target poisoning phenomenon [8]. This implies that the physical sputtering process of Ge becomes weaker than the growing process of carbon film on the Ge target. Since the $Ge_{1-x}C_x$ films at $R > 40\%$ cannot be obtained, the chemical bonding properties for the film grown at $R > 40\%$ will not be discussed any more.

Figure 2 shows the Raman spectra for the $Ge_{1-x}C_x$ films measured in the range 200–2000 cm^{-1}. A broad peak between 1000 and 1800 cm^{-1} is observed, which is a mixture

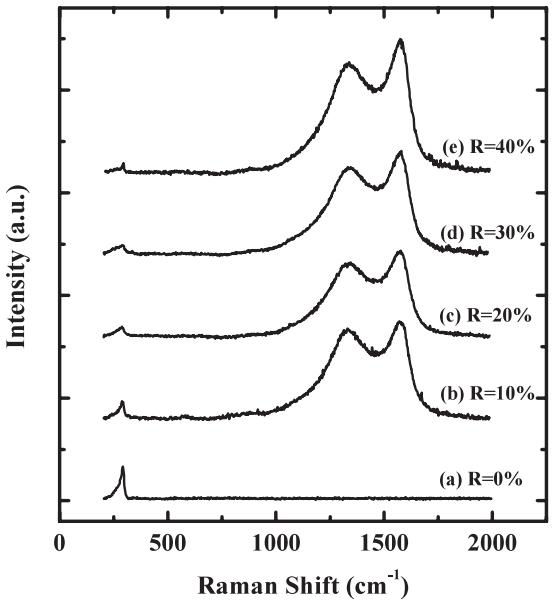

Figure 2. The Raman spectra for the $Ge_{1-x}C_x$ films deposited at different R.

of graphitic (G band) and disorder graphitic band (D band). The G peak at ∼1570 cm^{-1} is associated with the symmetric E_{2g} vibrational mode in graphite-like materials, while the D band at ∼1340 cm^{-1} is attributed to disorder-allowed phonon modes, which become Raman active as a result of destroying long-range order in amorphous graphitic materials [10]. In figure 2, the intensity of the band between 1000 and 1800 cm^{-1} increases with the increase of the R, which implies that the fraction of C–C bonds in the $Ge_{1-x}C_x$ films increases as CH_4 flow rate increases [17]. In addition, the Raman peak around 290 cm^{-1} originating from Ge–Ge TO (transverse optical) mode vibration is also observed clearly [10, 18]. This band becomes weaker as the R increases from 0 to 40%, which can be attributed to the decrease of the Ge content. Figure 3 shows the FTIR spectra for the $Ge_{1-x}C_x$ films measured in the range 400–4000 cm^{-1}. As expected, the pure Ge films (figure 3(a)) do not have any IR absorption peak because the Ge–Ge bonds are basically IR inactive. However, as the gas CH_4 is introduced gradually, the main absorption bands at ∼610, ∼1900 and ∼2900 cm^{-1} are clearly observed from curve (b) to curve (e). The absorption band at ∼610 cm^{-1} is related to the Ge–C stretching vibration [9, 16], the absorption band at ∼1900 cm^{-1} can be attributed to the Ge–H stretching mode [8, 9], while the absorption band at ∼2900 cm^{-1} is associated with C–H_n ($n = 1, 2, 3$) stretching modes [8, 9]. It can be seen clearly in figure 3 that the intensity of C–H_n ($n = 1, 2, 3$) increases gradually as R increases from 0 to 40%. Shinar [19] pointed out that the C–H bonds in the films were mainly obtained from the direct deposition of CH_n ($n = 1, 2, 3$) groups decomposed from methane. Thus, the increase of the fraction of C–H bonds in the $Ge_{1-x}C_x$ films should be due to the increase of the CH_n groups in the plasma as CH_4 flow rate increases.

Figure 4 displays the C 1s core energy spectra for $Ge_{1-x}C_x$ samples after Ar etching for 2 min as a function of R. The main features are related to carbon atoms bonded to germanium, hydrogen and carbon atoms. The features of C 1s spectra gradually change as the R increases, which implies that the chemical environment surrounding the incorporated C atoms is significantly influenced by R. The C 1s spectra show asymmetric line shape exhibiting a tailing toward higher binding energy and a doublet for R around 10%. These clear features

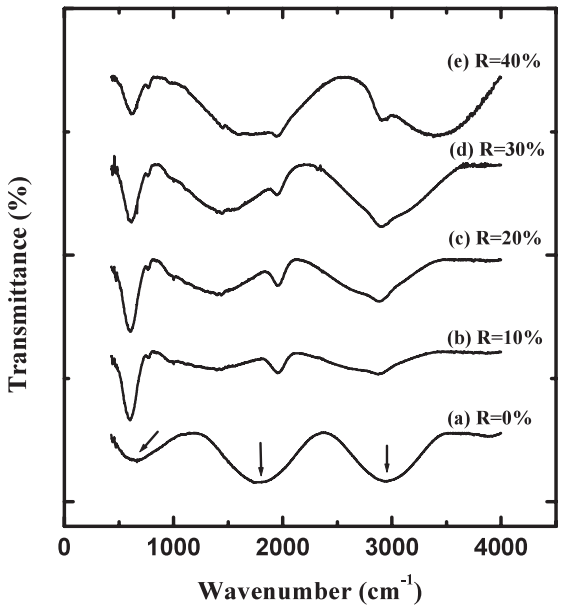

Figure 3. The FTIR spectra for the $Ge_{1-x}C_x$ films deposited at different R. The arrows denote interference effect in curve (a).

of C 1s spectra allow us to identify some contributions from the different chemical bonding between C atoms and C, Ge and H atoms. The C 1s spectrum in figure 4 could be well fitted using three Gaussian components, as shown in figure 5. The first component, at about 283.8 eV, is ascribed to Ge–C bonds in carbide forms [20], the second component, at about 284.6 eV, is ascribed to C–C bonds, and the third component, at about 285.7 eV, is associated with C–H_n bonds. A similar procedure has already been used in other compounds [21].

The integrated intensity of the peaks in figure 5 is plotted as a function of R, which is shown in figure 6. As R increases from 0 to 40%, the fraction of both C–H and C–C bonds increases (figures 6(a) and (b)). However, that of Ge–C bonds increases as R increases from 0 to 20%, and then decreases gradually as R increases from 20 to 40% (figure 6(c)). The change of the integrated intensity of the C–H_n peaks (figure 6(a)) is consistent with that of C–H_n absorption bands in the FTIR spectra, and the variation of the C–C bands (figure 6(b)) is similar to the one obtained by Raman measurement. In figure 6(c), the fact that the fraction of Ge–C bonds reaches its maximal value at about $R = 20\%$ means that the combining process of carbon and germanium atoms in the $Ge_{1-x}C_x$ network is sensitive to the variation of R. As we know, carbon atoms have the ability to enter the network with different hybridizations, the sp^3 and sp^2 being the most common. Much research showed that the hybridized configuration of carbon atoms was strongly influenced by the chemical environment surrounding the incorporated C atoms. For example, many research groups found in the a-SiC:H films [22–25] that silicon atoms could promote the formation of sp^3 carbon sites in the Si–C bonding, because silicon can only have sp^3 hybridization. For the Si-rich films carbon atoms mainly bond to silicon atoms in sp^3 configuration, whereas for the C-rich films carbon atoms preferentially combine to carbon in sp^2 configuration. In turn, the same phenomenon may take place in the $Ge_{1-x}C_x$ films, because germanium atoms also can only have sp^3 hybridization. In the low R region ($0\% < R < 20\%$), the $Ge_{1-x}C_x$ films present a high germanium content (Ge/C > 1.5), as shown in figure 1. In this scenario, sufficient germanium atoms may force their tetrahedral

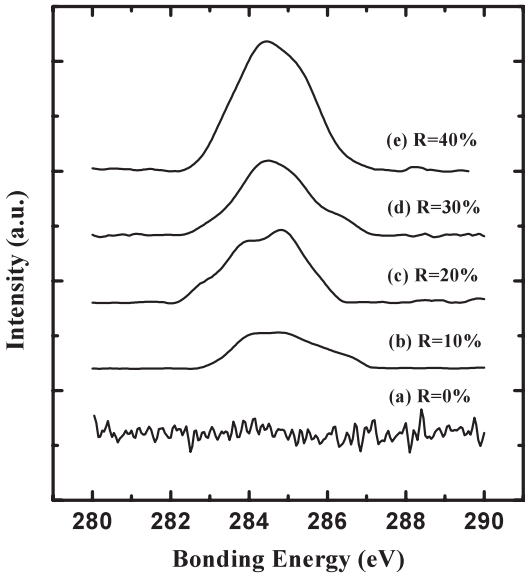

Figure 4. The XPS C 1s core energy spectra for the $Ge_{1-x}C_x$ films grown at different R.

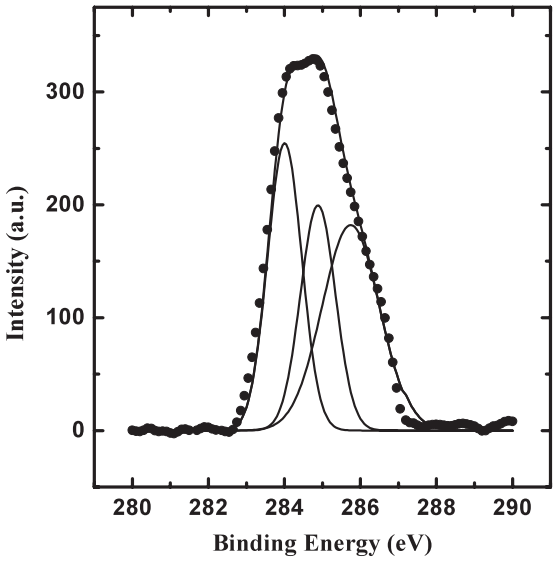

Figure 5. A typical C 1s spectrum for the $Ge_{1-x}C_x$ film grown at $R = 10\%$ can be well fitted using three Gaussian curves, which are ascribed to Ge–C, C–C and C–H bonds, respectively.

configuration upon carbon and lead to a dominant formation of tetrahedral carbon atoms. Consequently, as R increases from 0 to 20%, the number of sp^3 carbon atoms gradually increases and leads to the increase of Ge–C bonds, as shown in figure 6. However, as R increases from 20 to 40%, the effect of germanium atoms on the formation of tetrahedral carbon atoms fades away with decreasing Ge content. Accordingly, the number of sp^3 carbon atoms reduces, while that of sp^2 carbon atoms rapidly increases. As a result, the fraction of sp^2 C–C bonds rapidly increases, while that of Ge–C bonds decreases, as shown in figure 6.

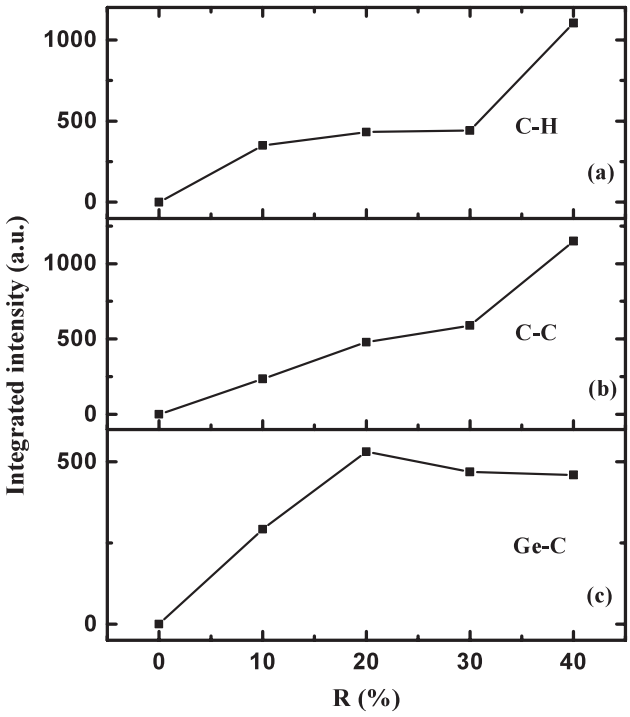

Figure 6. The integrated intensities of the three components in C 1s spectra for the $Ge_{1-x}C_x$ films as a function of R.

3.2. Optical and mechanical properties

Figure 7 shows the relationship between the refractive index n and the gas flow rate ratio (R) of $CH_4/(Ar + CH_4)$. The refractive index of the film prepared by a pure argon ($R = 0\%$) discharge is about 4.9 and corresponds to that of amorphous germanium film. As expected, with an increase in R the refractive index decreases monotonically, as shown in figure 7. It is known that the refractive index of the films depends on the composition and structure of the films. The composition analyses above indicate that germanium content of $Ge_{1-x}C_x$ films reduces and carbon content increases with increasing R, resulting in the formation of the structure more similar to a-C:H films. It has been confirmed that the refractive index of a-C:H films deposited under different processing conditions can be varied between 1.7 and 2.3 [26]. Therefore, it is understandable that the refractive index of the $Ge_{1-x}C_x$ film decreases with increasing CH_4 flow. The refractive index of the $Ge_{1-x}C_x$ films can be adjusted by changing the gas flow rate ratio of $CH_4/(Ar + CH_4)$ from 4.9 down to ≈2.4, which is of practical significance for designing and preparing multilayer IR coatings.

The optical gap E_g for the $Ge_{1-x}C_x$ film samples deposited at different R is shown in figure 8, according to the Tauc equation, determined by plotting $(\alpha h\nu)^{1/2}$ against the photon energy $h\nu$. It should be noted in figure 8 that E_g increases only in the range of $0\% < R < 20\%$, whereas it keeps almost constant for $R > 20\%$. The widening of the optical gap can be attributed to an increase in the number of stronger Ge–C bonds (bond energy is about 105 kcal mol^{-1}) created in the Ge network at the expense of the weaker Ge–Ge bonds (bond energy is about 65 kcal mol^{-1}) [4] as R increases from 0 to 20%. Nevertheless, the increase in hydrogen concentration with an increase in CH_4 flow may also be the other reason for this

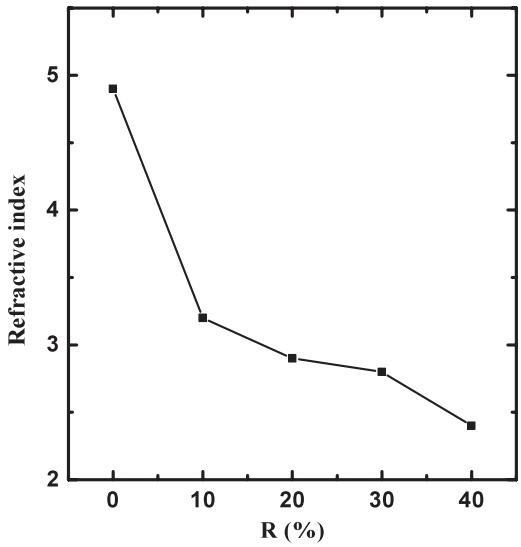

Figure 7. The refractive index of $Ge_{1-x}C_x$ films as a function of R.

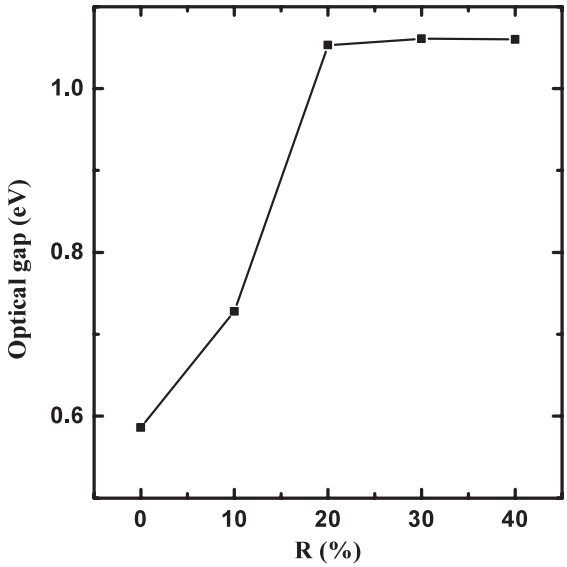

Figure 8. The optical gap E_g for $Ge_{1-x}C_x$ films as a function of R.

widening. However, for the $Ge_{1-x}C_x$ films deposited at high R ($20\% < R < 40\%$), the optical gap is almost constant, which can be ascribed to an increase in fraction of sp^2 C–C bonds as R increases. It is well known that π bonds contribute to closing the optical gap of a-C:H and a-$Si_{1-x}C_x$:H films. It has been found that for the hard carbon films the optical gap is related to the sp^3/sp^2 concentration ratio [27].

The Vickers hardness was measured at a relatively low 10 g load, and the $Ge_{1-x}C_x$ film thickness was larger than 1.2 μm. Figure 9 displays the dependence of the hardness on the gas flow rate ratio (R) of $CH_4/(Ar + CH_4)$. It can be seen that as R increases from 0 to 20% the

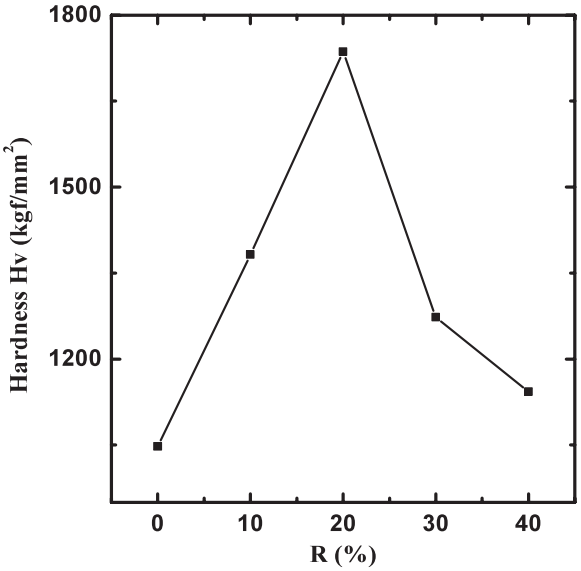

Figure 9. The Vickers microhardness for $Ge_{1-x}C_x$ films as a function of R.

hardness of the $Ge_{1-x}C_x$ films gradually increases and reaches a maximum value when R is at 20%, whereas it gradually decreases as R varies from 20 to 40%. As mentioned above, carbon atoms mainly bond to germanium atoms in sp^3 configuration for $R < 20\%$. As R increases from 0 to 20%, the germanium content of $Ge_{1-x}C_x$ films reduces and carbon content increases with increasing R, resulting in the formation of structure more similar to a diamond-like carbon. It has been confirmed that diamond-like carbon films have higher hardness compared to a-Ge films. Therefore, it is understandable that the hardness values increases with increasing R. However, as R varies from 20 to 40%, the hardness of $Ge_{1-x}C_x$ films gradually decreases. This fact may be related to an increase in the fraction of graphite-like sp^2 C–C bonding instead of diamond-like sp^3 Ge–C bonding when R is above 20%. This graphitization process has posed a strong limitation for the hardness improvement of a-C and a-SiC films, and the same problem is likely to be present for the $Ge_{1-x}C_x$ films. Moreover, the increase in $C–H_n$ bonding, as revealed by FTIR, may be the other reason for the reduction of the hardness as R increases, since the $C–H_n$ bonds are terminating bonds, which reduces the network coordination.

3.3. Applications of germanium carbide films

Concerning the application of the $Ge_{1-x}C_x$ films for antireflection and protection coatings of infrared windows, a $Ge_{1-x}C_x$ double-layer coating on ZnS substrate, deposited using RF reactive sputtering, has been developed in order to increase the optical transmittance of ZnS substrate in the wavelength region of 8–12 μm. In this double-layer system, the $Ge_{1-x}C_x$ film with a higher refractive index is preferred for the bottom layer and that with a lower refractive index is used for the top layer. From the above discussion, it has been known that lower R ($0\% < R < 20\%$) promotes the preparation of the $Ge_{1-x}C_x$ films with a higher refractive index, while higher R ($20\% < R < 40\%$) favours that of $Ge_{1-x}C_x$ film with a lower refractive index. Therefore, for the present double-layer $Ge_{1-x}C_x$ coating the desired refractive index of each layer can be achieved by adjusting R. During the preparation of the coating, the $Ge_{1-x}C_x$ layer (bottom layer) with a higher refractive index is 'graded' into that (top layer)

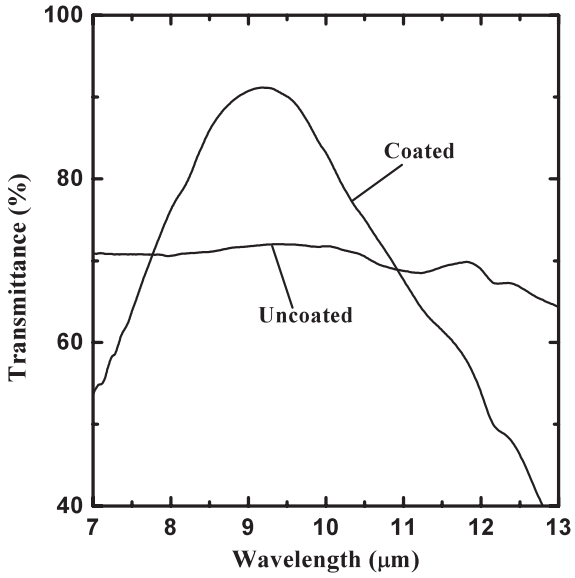

Figure 10. The IR transmittance spectra of the double-layer coating on the ZnS substrate.

with a lower refractive index by slowly changing the flow rate of methane and argon without stopping deposition. This processing has the advantage of preventing any well defined interface and the delamination when the coating is subjected to harsh conditions.

Figure 10 shows the IR transmittance spectra of the ZnS wafer coated on both sides with the double-layer coating in the 7–13 μm region. The measured refractive indices and thicknesses of both $Ge_{1-x}C_x$ layers are $n_1 = 3.89$, $d_1 = 602$ nm; $n_2 = 2.58$, $d_2 = 858$ nm. It can be seen from figure 10 that the IR transmittance for the coated ZnS wafer is significantly improved in the wavelength region of 8–12 μm. The maximum value of the IR transmittance of ZnS substrate wafer with the double-layer coating on both sides reaches 91%, which comes up to the theoretical value if the natural absorption of the $Ge_{1-x}C_x$ films is considered. In addition, the Vickers hardness measurements show that the the hardness of the ZnS substrate has been significantly improved by overcoating the double layer, and the hardness of the coated ZnS substrate (1277 kgf mm^{-2}) is approximately four times as high as that of the uncoated ZnS substrate (338 kgf mm^{-2}). It is of great importance for IR windows to be coated by durable protective anti-reflection films, because the high hardness coating offers the possibility for abrasion resistance. These results suggest that such a double-layer $Ge_{1-x}C_x$ can be used as an effective antireflection and protection coating for the ZnS IR window.

4. Conclusions

Germanium carbide ($Ge_{1-x}C_x$) films have been prepared by RF reactive sputtering a pure Ge(111) target at different flow rate ratios (R) of $CH_4/(CH_4 + Ar)$ in a discharge CH_4/Ar, and it has been found that the composition, chemical bonding, optical and mechanical properties of $Ge_{1-x}C_x$ films can be remarkably influenced by R. The content of germanium in the film gradually decreases with R increases from 0 to 40%, but when R is more than 40% the target-poisoning phenomenon occurs and the germanium atoms almost disappear in the film. In the range $0\% < R < 20\%$, the carbon atoms seem to enter the germanium network mainly in

the sp^3 configuration. The optical gap and hardness both gradually increase with increasing R, which can be mainly due to a consistent increase of sp^3 Ge–C bonds. However, in the range $20\% < R < 40\%$, the $Ge_{1-x}C_x$ films show more characteristics of graphitic-like films, which is associated with an increase in incorporation of sp^2 hybridized carbon atoms with increasing R. This graphitization process hinders the widening of the optical gap and leads to the consistent decrease in the hardness of $Ge_{1-x}C_x$ films with increasing R. Furthermore, a high efficiency antireflection $Ge_{1-x}C_x$ double-layer coating for ZnS windows has been developed for an infrared window. This double-layer coating on both sides of ZnS wafer can greatly enhance the IR transmittance in the interesting band of 8–12 μm. Meanwhile, this double-layer coating can also significantly improve the hardness of ZnS substrate, and the hardness of the coated ZnS substrate is approximately four times as high as that of the uncoated ZnS substrate, which suggests that such a double-layer $Ge_{1-x}C_x$ can be used as an effective antireflection and protection coating for a ZnS IR window.

Acknowledgments

Support from the Natural Science Foundation of China (grant Nos 50372024 and 50525204) and the Teaching and Research Award Programme for Outstanding Young Teachers in Higher Education Institutions (No 2002359) is acknowledged.

References

[1] Jilbert G H and Field J E 2000 *Wear* **243** 6
[2] Szmidt J, Gazicki-Lipman M, Szymanowski H, Mazurczyk R, Werbowy A and Kudla A 2003 *Thin Solid Films* **441** 192
[3] Tyczkowski J and Ledzion R 1999 *J. Appl. Phys.* **86** 4412
[4] Kumar S and Trodahl H J 1990 *Thin Solid Films* **193/194** 72
[5] Kumar S, Kashyap S C and Chopra K L 1988 *J. Non-Cryst. Solids* **101** 287
[6] White S B and McKenzie D R 1990 *J. Appl. Phys.* **68** 3194
[7] Gazicki M, Pirker K, Schallauer R, Fallmann W, Olcaytug F, Urban G, Jachimowicz A and Kohl F 1990 *Thin Solid Films* **187** 51
[8] Drüsedau T P, Annen A, Schröder B and Freistedt H 1994 *Phil. Mag.* B **69** 1
[9] Saito N, Nakaaki I, Yamaguchi T, Yoshioka S and Nakamura S 1995 *Thin Solid Films* **269** 69
[10] Mariotto G, Vinegoni C, Jacobsohn L G and Freire F L Jr 1999 *Diamond Relat. Mater.* **8** 668
[11] Vilcarromero J, Marques F C and Freire F L Jr 1998 *J. Appl. Phys.* **84** 174
[12] Maruyama T and Akagi H 1996 *J. Electrochem. Soc.* **143** 4087
[13] Mackowski J M, Cimma B and Pignard R 1992 *Proc. SPIE* **1760** 201
[14] Martin P W, Johnston J W and Bennett W D 1990 *Proc. SPIE* **1323** 291
[15] Zheng W T, Li J J, Wang X, Li X T, Jin Z S, Tay B K and Sun C Q 2003 *J. Appl. Phys.* **94** 2741
[16] Saito N, Yamaguchi T and Nakaaki I 1995 *J. Appl. Phys.* **78** 3949
[17] Gracin D, Bogdanović I, Borjanović V, Jakšić M, Pastuović Ž, Dutta J M, Vlahović B and Nemanich R J 2001 *Vacuum* **61** 303
[18] Kumeda M, Masuda A and Shimizu T 1998 *Japan. J. Appl. Phys.* **37** 1754
[19] Shinar J, Wu H S, Shinar R and Shanks H R 1987 *J. Appl. Phys.* **62** 808
[20] Bruce T, Bello I, Huang L J, Lau W M, High M, Strnad V and Panchhi P 1994 *J. Appl. Phys.* **76** 552
[21] Hicks S E, Fitzgerald A G, Baker S H and Dines T J 1990 *Phil. Mag.* B **62** 193
[22] Maruyama T and Mitani S 2003 *J. Non-Cryst. Solids* **319** 219
[23] Damasceno J C, Camargo S S Jr, Freire F L Jr and Carius R 2000 *Surf. Coat. Technol.* **133/134** 247
[24] Baia Neto A L, Santos R A, Freire F L Jr, Camargo S S Jr, Carius R, Finger F and Beyer W 1997 *Thin Solid Films* **293** 206
[25] Damasceno J C, Camargo S S Jr and Cremona M 2003 *Thin Solid Films* **433** 199
[26] Tsai H-C and Bogy D B 1987 *J. Vac. Sci. Technol.* A **5** 3287
[27] Chhowalla M, Robertson J, Chen C W, Silva S R P, Davis C A, Amaratunga G A J and Milne W I 1997 *J. Appl. Phys.* **81** 139